Journal of Pharmaceutical and Biomedical Analysis 212 (2022) 114640

Contents lists available at ScienceDirect

Journal of Pharmaceutical and Biomedical Analysis

journal homepage: www.journals.elsevier.com/journal-of-pharmaceutical-and-biomedical-analysis

Studies of interactions between fibronectin and a specific antibody against fibronectin using SPRi and QCM

Lukasz Oldak [a,b,*], Zenon Lukaszewski [c], Ewa Gorodkiewicz [b]

[a] Doctoral School of Exact and Natural Science, Faculty of Chemistry, Bioanalysis Laboratory, University of Bialystok, Ciolkowskiego 1 K, 15-245 Bialystok, Poland
[b] Bioanalysis Laboratory, Faculty of Chemistry, University of Bialystok, Ciolkowskiego 1 K, 15-245 Bialystok, Poland
[c] Faculty of Chemical Technology, Poznan University of Technology, pl. Sklodowskiej-Curie 5, 60-965 Poznan, Poland

ARTICLE INFO

Keywords:
Fibronectin
QCM
SPRi
Kinetics of interactions

ABSTRACT

Surface Plasmon Resonance Imaging (SPRi) and the Quartz Crystal Microbalance (QCM) technique were used to characterize the interactions between fibronectin and a specific monoclonal antibody against fibronectin. These techniques were used to investigate the formation of successive layers of the biosensor and how they affect the biosensor's response. The analytical response of both detectors to fibronectin concentration is linear in the range 5–100 ng/mL. The changes in mass on the surface of a quartz crystal covered with a layer of gold during biosensor formation were investigated with a QCM. The equilibrium constant was determined to be K_C = $1.22 \cdot 10^8$ dm^3/mol and the dissociation constant to be $K_D = 8.20 \cdot 10^{-9}$ mol/dm^3.

1. Introduction

The interaction between an immobilized antibody and an antigen is the basis for the construction of immunosensors. These interactions are incorporated in such methods for the determination of biomolecules as enzyme linked immunosensor assay (ELISA), chemiluminescence enzyme immunoassay (CLEIA), electrochemiluminescence immunoassay (ECLIA), chemiluminescent microparticle immunoassay (CMIA), Surface Plasmon Resonance (SPR) and Quartz Crystal Microbalance (QCM). Most of these methods use biosensors having a sandwich structure, with a secondary antibody conjugated with a label. The label enables the creation of an analytical signal. Among these techniques, only SPR and QCM are label-free, with the analytical signal created solely by the interaction of an antibody with a biomolecule.

The Surface Plasmon Resonance (SPR) technique is an optical method that examines changes in the reflection rate. These changes are due to the appearance of biological layers on the metal surface. A fraction of light falling at a specific angle interacts with plasmons (collective vibrations of free electron gas density). As a result of this impact, the intensity of reflected light is reduced. The result is a decrease in the amount of reflected light at this specific angle, called the SPR angle. With SPR, it is possible to monitor the interaction between biomolecules in real time without a label [1]. One of the variants of SPR is Surface Plasmon Resonance Imaging (SPRi). The essence of SPRi measurement is analogous to that of classical SPR. Classical SPR and SPRi differ in the recording of an analytical signal. In the case of classical SPR, the analytical signal is a change in the SPR angle depending on the increase in mass on the metal surface. In the case of SPRi, a CCD camera (detector) records changes in the brightness intensity of fields that correspond to the active areas on the metal surface. In other words, changes in the intensity of the reflected light are measured at a constant value of the beam incidence angle [2,3]. Using a non-fluidic array version of the SPRi technique, both quantitative and qualitative determination of different biomarkers in body fluids on the basis of an antibody marker is possible. Antibodies have been successfully used as receptors in biosensors for the determination of fibronectin (FN) [4] cathepsin S [5], CA125 [6] CEA [7], leptin [8] and papain [9].

A Quartz Crystal Microbalance (QCM) is a device that reacts to changes in thickness or weight per unit of quartz crystal surface. These changes are represented by changes in the resonant frequency of the quartz crystal [10]. In 1959, Sauerbrey demonstrated the relationship between the frequency of oscillation of a quartz crystal and the change in mass on its surface, as expressed by Eq. (1) [11]:

$$\Delta m = - \frac{\Delta f}{C_f} \quad (1)$$

* Corresponding author at: Doctoral School of Exact and Natural Science, Faculty of Chemistry, Bioanalysis Laboratory, University of Bialystok, Ciolkowskiego 1K, 15-245 Bialystok, Poland.
E-mail addresses: l.oldak@uwb.edu.pl (L. Oldak), zenon.lukaszewski@put.edu.pl (Z. Lukaszewski), ewka@uwb.edu.pl (E. Gorodkiewicz).

https://doi.org/10.1016/j.jpba.2022.114640
Received 11 August 2021; Received in revised form 25 January 2022; Accepted 30 January 2022
Available online 1 February 2022

where:

Δm – mass change [ng • cm^{-2}]
C_f – sensitivity factor of the crystal [0.0815 Hz • ng^{-1} • cm^{-2}]
Δf – change in frequency [Hz]

QCM has a wide range of applications, from thin layer deposition control to aerosol mass measurements. After applying the appropriate reconnaissance element to the quartz crystal, a very useful analytical device can be constructed. Such a sensor can be sensitive to a single compound or a class of compounds. For this reason, various biosensors are constructed with a QCM as the basic element, including immunosensors and DNA biosensors. With QCM it is also possible to study drugs and gaseous substances [12].

For investigation of the interaction between an antibody and a marker, fibronectin and an antibody against fibronectin were selected. A biosensor containing immobilized rabbit monoclonal anti-fibronectin antibody has been successfully used for the determination of the marker in blood plasma [4].

Apart from SPR and QCM, antibody–protein interactions can also be investigated using Ultraviolet–visible–near-infrared (UV-Vis-NIR) [13,14], Interference Spectroscopy Reflectometry (RIfS) [15,16], Bio-Layer Interferometry (BLI) [17,18], Surface-Enhanced Raman Scattering (SERS) spectroscopy [19,20], and Western Blot (WB) [21,22].

Fibronectin (FN) is an intermediary of many different cellular interactions with the extracellular matrix (ECM). It plays an important role in adhesion, migration, cell growth and differentiation. FN usually occurs as a dimer, composed of two almost identical subunits. The molar mass of FN is approximately 250 kDa. FN subunits are covalently connected near their C-ends via a pair of disulfide [23]. In mammals, FN occurs in various molecular forms: a soluble form, called plasma FN (PFN); and insoluble fibronectin, which occurs in two forms – one associated with the cell membrane and one which occurs in the ECM as a networking agent [24]. Over-expression of fibronectin and changes in its structure and concentration in body fluids may indicate the presence of certain disease units. Elevated levels of FN in blood plasma have been observed in patients with cancers such as gastric [25], colon [26], breast [27] and bladder cancer [28]. An increase in blood plasma FN has also been observed for rheumatic diseases [29] and coronary heart disease [30].

The aim of this work was to compare the behavior of an identical biosensor and its interaction with an analyte under conditions of SPRi and QCM measurements, as well as to compare the analytical characteristics for the two techniques. As in the available literature [31,32], we carried out measurements using both methods. However, we had the SPRi device working in a stationary mode and we prepared both methods to be used for the quantification of FN by calibrating them.

2. Material and methods

2.1. Chemical and biological reagents

The recombinant human fibronectin (FN); rabbit monoclonal anti-fibronectin antibody (anti-FN); N-hydroxysuccinimide (NHS); N-(3 dimethylamino-propyl)-N ethylcarbodiimidehydrochloride (EDC) and cysteamine were purchased in Sigma Aldrich (Germany). Carbonate buffer, pH= 8.50 and phosphate-buffered saline pH = 7.40 (PBS Buffer) were gained from Biomed Lublin (Poland). Ethanol 99.8% were obtained from POCh Gliwice (Poland).

2.2. Apparatus

SPRi measurements were made using a prototype SPRi apparatus constructed in the Bioanalysis Studio of the UwB Chemistry Department in collaboration with AC S.A., Bialystok, Poland. This device has a diode laser as a light source, with a wavelength of 635 nm and a maximum power of 8 mW (LP635-SF8, ThorLabs, Sweden), a collimator ($\lambda = 635$ nm, f = 35.41 mm, NA = 0.25 FC/PC Fiber Collimator, F810DC-635), a bezel (5x Achromatic Galilean Beam Expander, AR-coated, 400–650 nm, GBE05-A), a lens (0.243X Bi-Telecentric C-Mount Camera Lens for Sensor Formats up to 2/3", MVTC23024) and polarizers (Linear Polarizer with N-BK7 Protective Windows, 400–700 nm, LPVISE100-A – Φ1"). The measuring system also includes a glass prism (BK-7 glass), all angles of which are 60 degrees. The detector function is performed by a CCD camera with a 12-bit CCD sensor with a resolution of 1392 × 1040 pixels (Basler AG, Germany). The device is based on the Kretschmann configuration.

The study also used a quartz microbalance (Metrohm Autolab B.V., Netherlands) in conjunction with a potentiostat/galvanostat (Metrohm Autolab B.V. PGSTAT 302 N, Netherlands). The apparatus consists of a measuring cell of maximum volume 3 mL, made of polypropylene, having two O-rings, and between them a crystal with a resonant frequency of 6 MHz, on which a 10 nm layer of TiO_2 and a 100 nm layer of gold are sputtered. The crystal is double-sided, each side having an area of 0.361 cm^2. NOVA 2.1 software was used to control the device and analyze the received data.

2.3. SPRi measurements

Studies of interactions between fibronectin and a specific antibody were conducted using a previously constructed fibronectin-sensitive SPRi biosensor [4]. A monoclonal rabbit-specific anti-FN antibody was used as a receptor. A preprepared SPRi biosensor with an activated specific antibody to human fibronectin was applied successively to appropriate concentrations of standard solutions, which were left on its surface for 10 min to allow antibody–fibronectin interaction. The interaction took place at pH = 7.4 in a PBS buffer. Finally, the biosensor was washed with HBS-ES buffer and water. The buffer and water were removed from the chip surface by means of a vacuum.

2.4. QCM measurements

A biosensor for use with QCM was constructed in a similar way to the previously described fibronectin-sensitive biosensor. The first step was to form a self-organizing thiol cysteamine monolayer on the surface of the crystal. For this purpose, an alcoholic solution of cysteamine with a concentration of 20 mM was prepared. A quartz crystal was placed in the QCM cell, then the two parts of the cell were properly connected (there are two O-rings between them). The maximum volume of the cell is 3 cm^3. Then 2 cm^3 of MilliQ water was poured into the prepared cell, and the measurement of oscillation changes (Δf) of the quartz crystal covered with only a layer of gold was initiated. This measurement served as the basis (the zero value) for subsequent biological layers applied to the crystal. The water was next removed from the cell using a vacuum pump and the crystal was dried with an argon stream. A previously prepared cysteamine solution (2 cm^3) was poured in. The solution was left for at least 2 h to allow a cysteamine mono-layer to form on the surface of the crystal covered with a layer of gold. After 2 h, the cysteamine solution was removed with a vacuum pump. The crystal was rinsed with anhydrous ethyl alcohol and MilliQ water, and then dried with an argon stream. A measurement of Δf for the linker monolayer was performed. The next stage of the study was immobilization of the fibronectin-specific antibody. For this purpose, the antibody was activated with EDC and NHS solutions in a ratio of 1:1. A carbonate buffer of pH = 8.5 was used to maintain an appropriate reaction environment. The prepared antibody solution was placed in a microbalance cell and left for 1 h to allow the reaction to proceed. The Δf of the antibody was measured, and then the solution was removed from the microbalance cell. The final stage was the application of a protein – fibronectin – which was the examined analyte. The protein solution was placed in a microbalance cell and left for 10 min. This is the optimal time in which all predicted antibody–antigen interactions should take place. The Δf value was measured, and the test protein solution was removed from the cell.

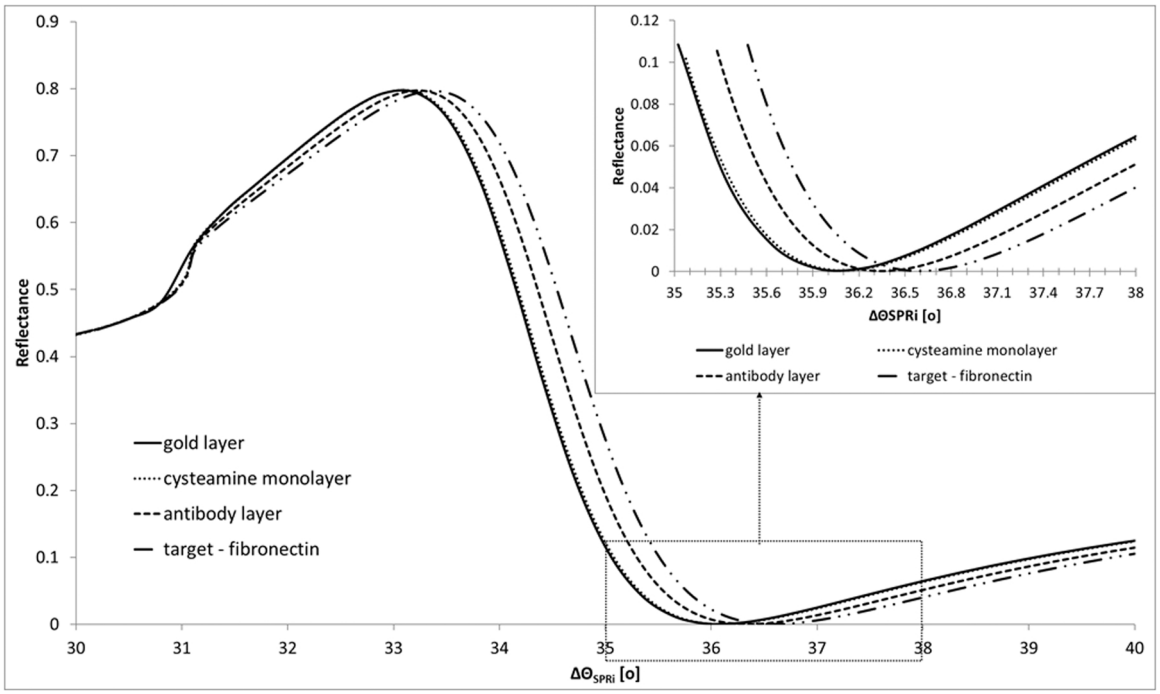

Fig. 1. SPR curves showing the formation of successive layers of the biosensor.

Table 1
Values of parameters used to model the SPR characteristics.

Prism	*triangular prism*		
Prism angle	*60°*		
Layer	**Thick [nm]**	**ε'**	**ε''**
BK-7	0	2.29	0
Chromium	1	-6.3	30
Gold	30	-12.45	1.3
Cysteamine	0.6	1	0
Anti-FN antibody	8	1.15	0
FN	12	1.18	0

3. Results and discussion

Changes in the analytical signal caused by the formation of subsequent layers of the biosensor were investigated, and a comparison of calibration curves for the SPR and QCM techniques was made.

3.1. SPRi measurements

The SPRi device used for the study operates on the Kretschmann configuration principle, which is based on the phenomenon of complete internal reflection. This occurs provided that the arrangement, consisting of a glass prism, a metal surface and a dielectric layer, is illuminated by a monochrome p-polarized beam of light. All of these conditions are met by exciting plasmons on top of the metal layer at an angle for which the wave vector of the photon is equal to the wave vector of surface plasmons [33]. A quantitative description of the SPR curves can be obtained by solving the Fresnel equations, which relate to the reflectance of p-polarized light in a multilayer system such as that involved in the construction of this biosensor [34]. In Fig. 1, SPR curves illustrate the process of formation of successive layers on the gold surface, as illustrated by the shifts in the SPR angle after each subsequent biosensor layer (cysteamine, antibody, fibronectin) has been formed. The curves shown were plotted using software to simulate the optical fit (WinSpall, version 3.02).

In Table 1, we have given the values of the parameters used to model the SPR characteristics in order to fit them to the experimental results.

A gradual shift in the SPR angle by approximately 0.6 degrees is observed, with a shift of approximately 0.2 degrees caused by the interaction between the immobilized antibody and fibronectin.

The dependence of the analytical signal on fibronectin concentration in the non-fluidic array version of the SPRi technique was investigated in the range 5–300 ng/cm^3. This relationship is shown in Fig. 2.

A plateau is observed above a concentration of 100 ng/cm^3, indicating maximum protein saturation of all available receptor sites on the biosensor surface. The analytically useful range is in the range of concentrations 5–100 ng/cm^3.

3.2. QCM measurements

The formation of subsequent layers on the gold surface was confirmed using the QCM technique. Before measurement of a frequency, the processing liquid used for the formation of a particular layer was removed and replaced by water. Changes in frequency were measured, and then the next layer was created. The value measured for uncovered gold was fixed as the zero value. The formation of subsequent layers is shown in Fig. 3. Layers of cysteamine, antibody and finally fibronectin are distinctly visible. Values of time corresponding to particular steps represent the time necessary to achieve a stable frequency value.

The dependence of the analytical signal on fibronectin concentration in the QCM technique was investigated in the range 5–300 ng/cm^3. The same solutions were used as for the SPRi measurements. The calibration curve obtained is shown in Fig. 4.

The analytically useful linear range is identical to that obtained in the case of SPRi (5–100 ng/cm^3). Both SPRi and QMC calibration curves have $R^2 = 0.999$.

Comparing the changes caused by the formation of successive layers of the biosensor as determined by the SPRi technique (Fig. 1) and by the QCM (Fig. 3), it is clear that the QCM indicates these changes more distinctly. The immobilization of cysteamine causes a shift by approximately 50 Hz in the QCM case (Fig. 3), while in SPR, the curves for bare gold and cysteamine (Fig. 1) are almost identical. The analytical signal created by the capture of fibronectin causes a change in the QCM signal by approximately 70 Hz (see Fig. 3) and a change in the SPR signal by

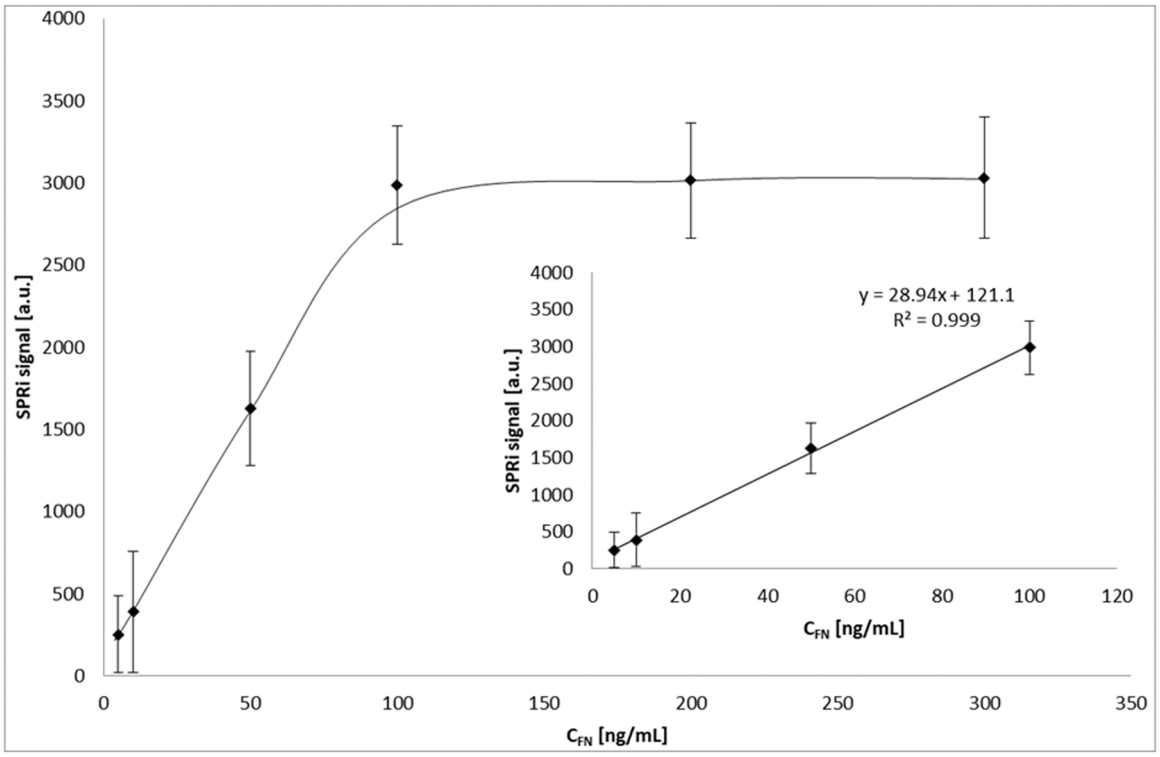

Fig. 2. Calibration curve of fibronectin as measured by the SPRi technique: the full-range curve and the analytically useful range. $C_{antibody} = 4\ \mu g/cm^3$, pH.= 7.40.

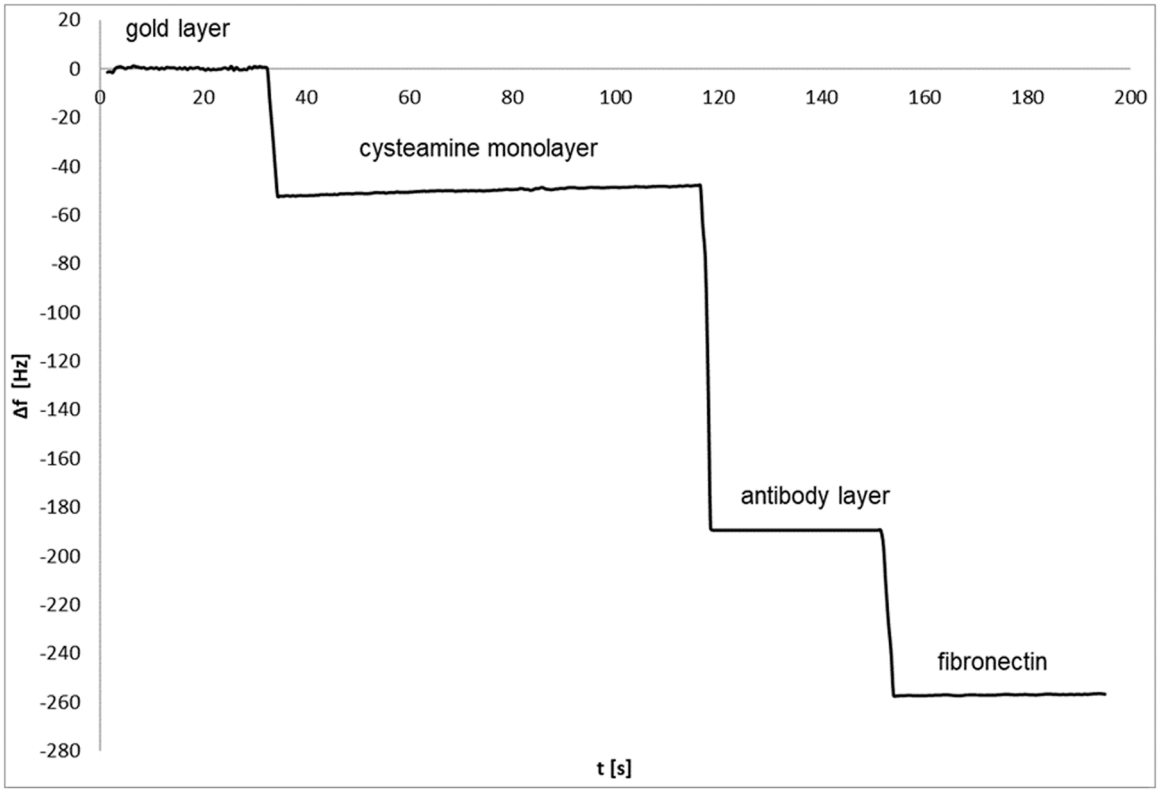

Fig. 3. Changes in the frequency of oscillation of the quartz crystal corresponding to the formation of successive biosensor layers.

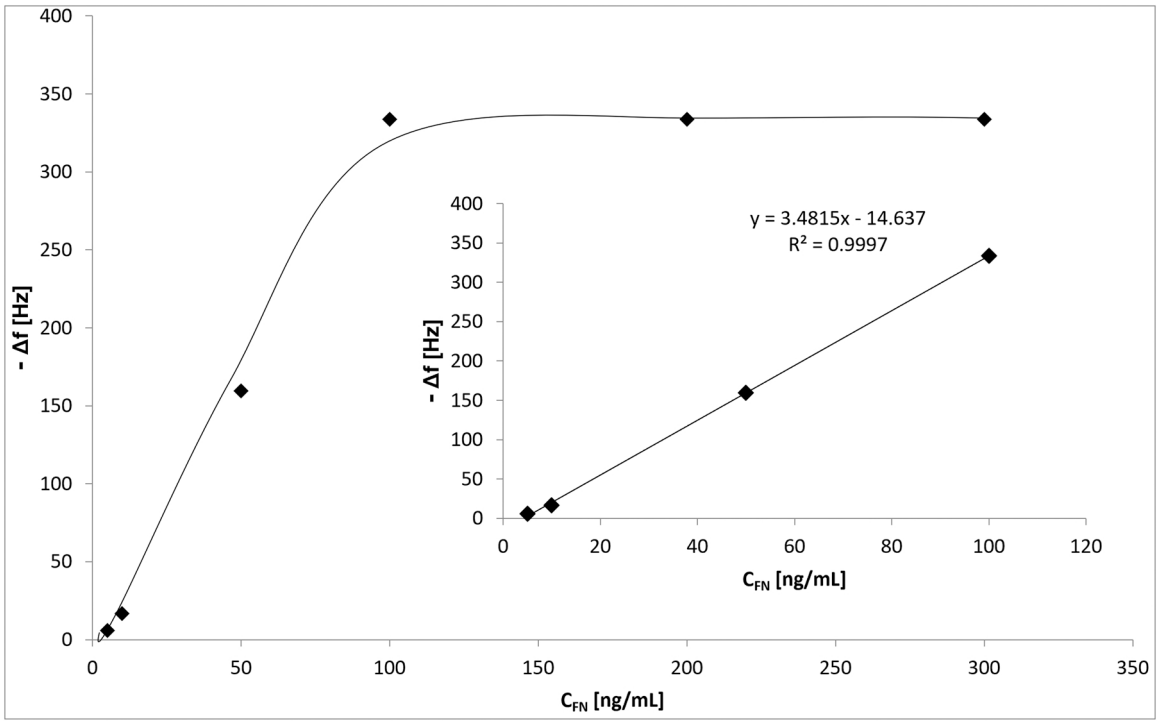

Fig. 4. Calibration curve for fibronectin as measured by the QCM technique: the full-range curve and the analytically useful range. $C_{antibody} = 4$ μg/cm^3, pH= 7.40.

Table 2
Characteristics of antibody–fibronectin interactions, determined by QCM measurements.

Part of biosensor	Δm [ng]	% Δm	K_C [dm^3 /mol]	K [mol/dm ^{3}]
Parameter			antibody - fibronectin	
cysteamine	0.211	0.005	$1.22 \cdot 10^8$	$8.20 \cdot 10^{-9}$
antibody	0.889	2.79		
fibronectin	1.137	7.58		

only approximately 0.3 degrees. However, the SPR signal converted to an image by the SPRi technique creates an analytical signal similar to that obtained by the QCM technique (compare Figs. 2 and 4).

The QCM technique enables the determination of an equilibrium constant. Changes in mass due to deposition of successive layers on the surface of the quartz crystal were also investigated, and the percentage relationship between these changes was determined. On this basis the equilibrium constant (K_C) and the dissociation constant (K_D) for the antibody–fibronectin complex were determined. The results are shown in Table 2.

The high value of the equilibrium constant is evidence of strong interaction between fibronectin and the rabbit monoclonal antibody against fibronectin. A similar study has not been conducted so far. However, it has been shown that FN binding to low molecular weight fucoidan (LMWF) alleviates kidney damage in diabetic nephropathy by binding to FN and inhibiting the pathway of appropriate interactions. Using the SPR, the K_D of LMWF and FN binding was determined, the value of which was equal to $K_D = 453{,}7$ μmol/L ($4.537 \cdot 10^{-4}$ mol/dm^3) [35]. We calculated the mass changes (Δm) resulting from the attachment of subsequent molecules. The lowest Δm value was observed when cysteamine was attached to the gold surface, but this result should not be alarming as cysteamine is a small chemical structure with a molecular weight of M = 77.15 g/mol. The biggest difference was made by the FN attachment (M = ~ 250 kDa) and confirmed its interaction with the antibody.

4. Summary

We attempted to construct a biosensor sensitive to FN using QCM as a kind of detection, which we then compared with the previously constructed SPRi biosensor, but after recalibration of the method. In both cases, the linear range of the calibration curves is between 5 and 100 ng/mL. Using QCM, we attempted to determine the K_C and K_D of the specific antibody-FN complex. We also calculated the mass changes on the crystal surface resulting from the appropriate bonds between the individual substances. SPRi and QCM were also used to confirm the formation of subsequent layers of the biosensor. For SPRi, we simulated SPR curves based on the obtained experimental data (Fig. 1), while for QCM we made a graph of frequency changes over time, which shows the process of attachment of subsequent substances during the construction of the biosensor (Fig. 3). Both graphs confirm that during the conducted research, successive substances being the relevant components of the biosensor were successively bound with the appropriate remaining substances.

The comparison of both methods gives us a suggestion that an identically constructed biosensor sensitive to FN can cooperate with both SPRi and QCM, giving the same working range of the calibration curve, which does not require special preparation of the test sample when changing the analytical method.

CRediT authorship contribution statement

Oldak L: Data curation, Investigation, Formal analysis, Writing – original draft. **Lukaszewski Z:** Writing – review & editing. **Gorodkiewicz E:** Conceptualization, Supervision.

Declaration of Competing Interest

The authors declare that they have no known competing financial interests or personal relationships that could have appeared to influence the work reported in this paper.

Acknowledgement

This article has received financial support from the Polish Ministry of Education and Science under subsidy for maintaining the research potential of the Faculty of Chemistry, University of Bialystok.

References

[1] P. Jain, D. Arora, S.C. Bhatla, Surface plasmon resonance based recent advances in understanding plant development and related processes, Biochem. Anal. Biochem. 05 (2016), https://doi.org/10.4172/2161-1009.1000300.
[2] E.A. Smith, R.M. Corn, Surface plasmon resonance imaging as a tool to monitor biomolecular interactions in an array based format,, Appl. Spectrosc. 57 (2003) 320A–332A, https://doi.org/10.1366/000370203322554446.
[3] E. Gorodkiewicz, Z. Lukaszewski, Recent progress in surface plasmon resonance biosensors (2016 to mid-2018), Biosensors 8 (2018) 1–18, https://doi.org/10.3390/bios8040132.
[4] A. Sankiewicz, L. Romanowicz, M. Pyc, A. Hermanowicz, E. Gorodkiewicz, SPR imaging biosensor for the quantitation of fibronectin concentration in blood samples, J. Pharm. Biomed. Anal. 150 (2018) 1–8, https://doi.org/10.1016/j.jpba.2017.11.070.
[5] L. Oldak, A. Sankiewicz, B. Żelazowska-Rutkowska, B. Cylwik, Z. Lukaszewski, M. Skoczylas, E. Gorodkiewicz, Two SPRi biosensors for the determination of cathepsin S in blood plasma, Talanta 225 (2021), 121900, https://doi.org/10.1016/j.talanta.2020.121900.
[6] B. Szymańska, Z. Lukaszewski, K. Hermanowicz-Szamatowicz, E. Gorodkiewicz, A biosensor for determination of the circulating biomarker CA125/MUC16 by surface plasmon resonance imaging, Talanta 206 (2020), 120187, https://doi.org/10.1016/j.talanta.2019.120187.
[7] B. Szymanska, Z. Lukaszewski, K. Hermanowicz-Szamatowicz, E. Gorodkiewicz, An immunosensor for the determination of carcinoembryonic antigen by surface plasmon resonance imaging, Anal. Biochem. 609 (2020), 113964, https://doi.org/10.1016/j.ab.2020.113964.
[8] A. Sankiewicz, A. Hermanowicz, A. Grycz, Z. Łukaszewski, E. Gorodkiewicz, An SPR imaging immunosensor for leptin determination in blood plasma, Anal. Methods 13 (2021) 642–646, https://doi.org/10.1039/d0ay02047h.
[9] E. Gorodkiewicz, The surface plasmon resonance imaging sensor for papain based on immobilized cystatin, Protein Pept. Lett. 14 (2007) 443–445, https://doi.org/10.2174/092986607780782803.
[10] N.L. Bragazzi, D. Amicizia, D. Panatto, D. Tramalloni, I. Valle, R. Gasparini. Quartz-Crystal Microbalance (QCM) for Public Health: An Overview of Its Applications, First ed.,, Elsevier Inc., 2015, https://doi.org/10.1016/bs.apcsb.2015.08.002.
[11] G. Sauerbrey, Verwendung von Schwingquarzen zur Wägung dünner Schichten und zur Mikrowägung, Z. Für Phys. 155 (1959) 206–222, https://doi.org/10.1007/BF01337937.
[12] C.K. O'Sullivan, G.G. Guilbault, Commercial quartz crystal microbalances - theory and applications, Biosens. Bioelectron. 14 (1999) 663–670, https://doi.org/10.1016/S0956-5663(99)00040-8.
[13] S.C.B. Gopinath, R. Kumaresan, K. Awazu, M. Fujimaki, M. Mizuhata, J. Tominaga, P.K.R. Kumar, Evaluation of nucleic acid duplex formation on gold over layers in biosensor fabricated using Czochralski-grown single-crystal silicon substrate, Anal. Bioanal. Chem. 398 (2010) 751–758, https://doi.org/10.1007/s00216-010-3994-z.
[14] R.N. Clark, T.L. Roush, Reflectance spectroscopy: quantitative analysis techniques for remote sensing applications, J. Geophys. Res. 89 (1984) 6329–6340, https://doi.org/10.1029/JB089iB07p06329.
[15] F. Gesellchen, B. Zimmermann, F.W. Herberg, Direct optical detection of protein-ligand interactions., Methods in Molecular Biology (Clifton, N.J.). 305 2005, pp.17–46. https://doi.org/10.1385/1–59259-912–5:017.
[16] W. Qian, D. Yao, F. Yu, B. Xu, R. Zhou, X. Bao, Z. Lu, Immobilization of antibodies on ultraflat polystyrene surfaces, Clin. Chem. 46 (2000) 1456–1463, https://doi.org/10.1093/clinchem/46.9.1456.
[17] R.L. Petersen, Strategies using bio-layer interferometry biosensor technology for vaccine research and development, Biosensors 7 (2017) 49, https://doi.org/10.3390/bios7040049.
[18] G.C. Barnard, M.D. Hougland, Y. Rajendra, High-throughput mAb expression and purification platform based on transient CHO, Biotechnol. Prog. 31 (2015) 239–247, https://doi.org/10.1002/btpr.2012.
[19] S. Nie, S.R. Emory, Probing single molecules and single nanoparticles by surface-enhanced Raman scattering, Science 275 (1997) 1102–1106, https://doi.org/10.1126/science.275.5303.1102.
[20] K.W. Kho, U.S. Dinish, A. Kumar, M. Olivo, Frequency shifts in SERS for biosensing, ACS Nano 6 (2012) 4892–4902, https://doi.org/10.1021/nn300352b.
[21] M.G. Hossain, K. Ueda, Investigation of a novel hepatitis B virus surface antigen (HBsAg) escape mutant affecting immunogenicity, PLoS ONE 12 (2017) 1–22, https://doi.org/10.1371/journal.pone.0167871.
[22] M.R. Golden, R. Ashley-Morrow, P. Swenson, W.R. Hogrefe, H.H. Handsfield, A. Wald, Herpes simplex virus type 2 (HSV-2) Western blot confirmatory testing among men testing positive for HSV-2 using the focus enzyme-linked immunosorbent assay in a sexually transmitted disease clinic, Sex. Transm. Dis. 32 (2005) 771–777, https://doi.org/10.1097/01.olq.0000175377.88358.f3.
[23] R. Pankov, K.M. Yamada, Fibronectin at a glance, J. Cell Sci. 115 (2002) 3861–3863, https://doi.org/10.1242/jcs.00059.
[24] R.O. Hynes, The dynamic dialogue between cells and matrices: implications of fibronectin's elasticity, Proc. Natl. Acad. Sci. USA 96 (1999) 2588–2590, https://doi.org/10.1073/pnas.96.6.2588.
[25] L. David, J.M. Nesland, R. Holm, S.-Simoes Manuel, Expression of laminin, collagen IV, fibronectin, and type IV collagenase in gastric Carcinoma an immunohistochemical study of 87 patients, Cancer 73 (1994) 518–527.
[26] N. Saito, H. Nishimura, S. Kameoka, Clinical significance of fibronectin expression in colorectal cancer, Mol. Med. Rep. 1 (2008) 77–81.
[27] E. Ruiz-Garcia, V. Scott, C. MacHavoine, J.M. Bidart, L. Lacroix, S. Delaloge, F. Andre, Gene expression profiling identifies fibronectin 1 and CXCL9 as candidate biomarkers for breast cancer screening, Br. J. Cancer 102 (2010) 462–468, https://doi.org/10.1038/sj.bjc.6605511.
[28] O.F. Abdul-rasheed, N.K. Habash, U. Al-nasiri, Iraqi JMS, 2014.
[29] N. Mete, M. Mete, Plasma fibronectin and urine glycosaminoglycane levels in rheumatic diseases, Turk. J. Med. Sci. 28 (1998) 437–442.
[30] K.S. Song, H.K. Kim, W. Shim, S.H. Jee, Plasma fibronectin levels in ischemic heart disease, Atherosclerosis 154 (2001) 449–453, https://doi.org/10.1016/S0021-9150(00)00490-1.
[31] E. Makhneva, Z. Farka, P. Skládal, L. Zajíčková, Cyclopropylamine plasma polymer surfaces for label-free SPR and QCM immunosensing of Salmonella, Sens. Actuators B Chem. 276 (2018) 447–455, https://doi.org/10.1016/J.SNB.2018.08.055.
[32] C. Ayela, F. Roquet, L. Valera, C. Granier, L. Nicu, M. Pugnière, Antibody–antigenic peptide interactions monitored by SPR and QCM-D: A model for SPR detection of IA-2 autoantibodies in human serum, Biosens. Bioelectron. 22 (2007) 3113–3119, https://doi.org/10.1016/J.BIOS.2007.01.020.
[33] E. Kretschmann, H. Raether, Radiative decay of non radiative surface plasmons excited by light, Z. Fur Naturforsch. Sect. A J. Phys. Sci. 23 (1968) 2135–2136, https://doi.org/10.1515/zna-1968-1247.
[34] A.W. Peterson, M. Halter, A.L. Plant, J.T. Elliott, Surface plasmon resonance microscopy: achieving a quantitative optical response, Rev. Sci. Instrum. 87 (2016) 1–20, https://doi.org/10.1063/1.4962034.
[35] J. Wang, Q. Zhang, S. Li, Z. Chen, J. Tan, J. Yao, D. Duan, Low molecular weight fucoidan alleviates diabetic nephropathy by binding fibronectin and inhibiting ECM-receptor interaction in human renal mesangial cells, Int. J. Biol. Macromol. 150 (2020) 304–314, https://doi.org/10.1016/J.IJBIOMAC.2020.02.087.